Regular Article

ORGANIC CHEMISTRY RESEARCH
Published by the
Iranian Chemical Society
www.orgchemres.org

***Org. Chem. Res.**, Vol. 6, No. 2, 219-232, September 2020.*
DOI: 10.22036/org.chem.2019.204444.1220

ZnO@zeolite-Y Mesoporous as an Eco-friendly and Efficient Nanocatalyst in the Three-component Synthesis of 2-Amino-benzochromenes

M. Kalhor[a,*], M. Bigdeli[a], S.A. Mirshokraie[a] and H. Moghanian[b]

[a]*Department of Chemistry, Payame Noor University, 19395-4697, Tehran, Iran*

[b]*Department of Chemistry, Dezful Branch, Islamic Azad University, Dezful, Iran*

(Received 8 October 2019, Accepted 28 December 2019)

A streamlined and efficient method for the synthesis of 2-amino-4*H*-chromenes is achieved by one-pot three-component reaction of aldehydes, 2-naphthol and malononitrile in the presence of ZnO nanoparticles loaded on zeolite-Y (ZnO@zeolite-Y) as a highly active catalyst under solvent-free conditions. ZnO@zeolite-Y was successfully prepared *via* hydrothermal technique and its structure was confirmed using nanoscale-like identification techniques included FT-IR, XRD, FE-SEM, EDX analyses and BET surface area measurements. The higher environmental compatibility and sustainability factors such as reusability of the catalyst as an important principle in green chemistry, use of solvent-less technique as a green synthetic approach and easy isolation of the product along with good yields make the present protocol a true green process for the synthesis of chromenes compared to conventional methods.

Keywords: ZnO nanoparticles, Zeolite-Y, Nanocatalyst, Multi-component synthesis, 2-Amino-4*H*-benzochromene

INTRODUCTION

In the recent years, crystalline porous materials have attracted increasing interest due to their applications in petrochemical, environmental technologies and in chemical reactions particularly for catalytic strategies. These porous compounds include zeolites, ordered mesoporous silica, and metal-organic frameworks. The main features for these materials are high adsorption capacity, active sites with different strengths, uniform channels and cavities, and electronic properties [1]. Among them, the zeolites have recently considered as heterogeneous catalysts or ideal supports for homogeneous catalysts due to their high surface area, high thermos-stability, nanoporous crystalline structure, persistence in all organic solvents, no waste or disposal problems, less or no corrosion, easy set-up of continuous processes, *etc.* [2]. In this regard, so far several reviews have been reported on their synthesis and application [3]. Therefore, they can be applied as a green and suitable support for various transition metal salts, metal ions and metal oxides in catalytic heterogeneous systems [4,5].

Metal oxide/zeolite nanostructures have been employed in catalytic processes for a variety of chemical reactions. These hybrid materials can be potential candidate for improved catalytic systems. Since zeolites as supports possess a generous surface area for high dispersion of nanocatalysts, well-defined arrays of channels and high porosity structure for maximum reactant contact, improve the electrical and structural properties of transition metal oxides to facilitate electron transport during chemical reactions and appropriate interaction of catalyst nanoparticles and the inorganic support for stable catalytic activity [6,7]. On the other hand, zinc oxide (ZnO) as a useful and efficient catalyst has been explored for organic conversions. In practical applications, the use of ZnO nanoparticles with a broad surface area has led to the development of their catalytic activities. However, these nanosized particles have limitations, including the problem of the separation of catalysts at the end of the processes and the aggregation of nanoparticles. To solve these problems, one interesting alternative is using ZnO supported on inert

*Corresponding author. E-mail: mekalhor@gmail.com

or active materials like zeolites that improves the catalytic efficiency and shows easy recovery by simple filtration and avoidance of aggregation of metal oxide nanoparticles [8-10]. ZnO loaded zeolites have not been investigated in the synthesis of chromene heterocycles, though they have been used for a variety of catalytic applications such as photocatalytic reactions [4,7], synthesis of benzothiazole derivatives and methane activation [8,11].

Synthesis of heterocycles with biological and pharmacological activities has widely been explored by chemists and pharmacists [12,13]. Among the wide range of heterocycles, chromenes and their structural analogues are privileged scaffolds in the synthesis of pharmacological and biological molecules [14,15]. Among the important chromene heterocycles, the synthesis of 2-amino-4*H*-chromenes and their derivatives have attracted increasing attention due to their diverse biological activities such as antitumor [16], mutagenicity [17], sex pheromone [18], antimicrobial [19], antiproliferative [20], cancer therapy and central nervous system activity [21].

Due to the importance of these medicinal applications, various strategies have been developed for the synthesis of 2-amino-4*H*-chromenes by cyclization of an aldehyde, malononitrile (or ethyl cyanoacetate), and enolizable C-H activated acidic compounds [22]. Numerous modified methods have been introduced for the synthesis of 2-amino-4*H*-chromenes using different catalysts such as N,N-dimethylaminoethyl benzyldimethylammonium chloride [23], cetyltrimethylammonium chloride/bromide [24], aminosilane modified Fe_3O_4 nanoparticles [22], hydrotalcite [25], MgO nanoparticles [26], heteropolyacid [27], DBU [28], supported imidazolium ionic liquid [29], $(BMIm)BF_4$ [30], Pd Ru/graphene oxide [31], and various conditions like ultrasound synthesis [32], solvent-free process [33], and microwave technique [34]. Most of these procedures reported suffer from the harsh reaction conditions and high temperature required, long reaction time and unsatisfactory yields, different isolation process and complex reaction pathway, use of organic solvents and catalyst recovery problem. Therefore, it is still needed to develop environmentally friendly techniques and the use of green and effective nanocatalysts for the synthesis of these heterocycles.

To gain further insight into the catalytic activates of the modified zeolite-Y in a heterocyclic synthesis [35-37], herein we would like to report ZnO@zeolite-Y as a valuable and reusable nanocatalyst for the synthesis of 2-amino-4*H*-chromenes by a one-pot reaction of various aldehydes, malononitrile, and 2-naphtol at 110 °C under solvent-free conditions.

EXPERIMENTAL

Chemicals in high purity were purchased from Merck, Fluka and Aldrich companies with commercial grade. Melting points (°C) were determined in an open-glass capillary using an electro-thermal digital melting point apparatus and were uncorrected. ^{1}H NMR (400) and ^{13}C NMR (100) spectra were measured using a Brucker Avance spectrometer operating at 250 and 100 MHz for proton and carbon-13, respectively in DMSO-d_6 and $CDCl_3$ with TMS as an internal standard. FT-IR spectra of all the compounds were measured on a Unicom Galaxy Series FT-IR 5000 spectrophotometer in the range 400-4000 cm^{-1} as KBr pellets. Progress of the catalytic process was monitored by thin layer chromatography (TLC) using silica gel plates in the elven system *n*-hexan-EtOAc (v/v = 7:3). Nanocomposites based zeolite-Y were characterized using a Holland Philips Xpert X-ray powder diffraction (XRD) diffractometer (CuK, radiation, λ = 0.154056 nm), at a scanning speed of 2°/min from 10° to 100° (2θ). Field emission-scanning electron microscopic (FE-SEM) images were performed on a *Zeiss* Sigma FE-SEM that it equipped with energy dispersive X-ray spectrometer (EDX). Adsorption/desorption isotherms were obtained in static mode, and N_2 was used as the analysis gas at 77 K. For zeolite-based samples, the BET surface area was obtained on a BElSORP Mini.

Preparation of the ZnO@zeolite-Y Nanocomposites

Zn@zeolite-Y was prepared using hydrothermal method by mixing $ZnCl_2.2H_2O$ (0.172 g, 1 mmol) aqueous solution with zeolite-Y (0.05 g) under sonication. The mixture was stirred for 30 min. Next, ammonia solution (25%, 2-3 ml) was added into the suspension to pH 11 under ultrasound irradiation and the mixture was stirred for 90 min at

50-60 °C. Thereafter, the white $Zn(OH)_2$ precipitate was separated by centrifuging and washed with deionized water and dried at 50-60 °C in oven. Finally, the sample was heated at 500 °C for 2 h to afford ZnO@zeolite-Y nanostructures.

General Procedure for the Catalytic Synthesis of 2-Amino-4H-chromenes

A mixture of aldehyde (1 mmol), 2-naphtol (1 mmol), malononitrile (1.2 mmol) and ZnO@zeolite-Y (0.05 g) were added to a 50 ml flask and the mixture was stirred at 110 °C under solvent-free conditions for the pre-determind time (Table 2). After completion of the reaction (indicated by TLC; *n*-hexane:ethyl acetate, 8:2), the solidified mixture washed with H_2O/EtOH (1:1) (2 × 10 ml) and dissolved in hot EtOH. The insoluble catalyst was separated by filtration and the pure product was crystallized from EtOH in high yield.

Spectral Data for some of the Product

3-Amino-1-(2-methoxyphenyl)-1H-benzo[f] chromene-2-carbonitrile (4c) (Table 2, Entry 3). FTIR (KBr) υ: 3458, 3345, 3123, 2965, 2183, 1649, 1592, 1473, 1438, 1234, 1179, 1024, 1011, 814, 748, 527, 338 cm^{-1}. ^1H NMR (400 MHz, DMSO-d_6) δ_H 8.01-7.98 (m, 2H, H-Ar), 7.84 (d, 1H, J = 8.24 Hz, H-Ar), 7.55-7.49 (m, 2H, H-Ar), 7.41 (d, 1H, J = 8.92 Hz, H-Ar), 7.20 (m, 1H, H-Ar), 7.13 (d, 1H, J = 8.88 Hz, H-Ar), 6.97-6.84 (m, 4H, NH_2 and H-Ar), 5.68 (s, 1H, CH), 3.97 (s, 3H, OMe) ppm; ^{13}C NMR (100 MHz, DMSO-d_6) δ_C 160.1, 155.6, 147.1, 133.5, 130.6, 130.2, 129.1, 128.5, 128.4, 127.9, 127.1, 124.8, 122.8, 121.0, 120.4, 116.6, 115.8, 111.6, 56.8, 55.9, 31.7 ppm.

3-Amino-1-(2,6-dichlorophenyl)-1H-benzo[f] chromene-2-carbonitrile (4n) (Table 2, Entry14). FTIR (KBr) υ: 3462, 3336, 2187, 1662, 1593, 1517, 1493, 1409, 1235, 1185, 1084, 1028, 814, 752, 696, 611, 559, 490 cm^{-1}. ^1H NMR (400 MHz, DMSO-d_6) δ_H 8.03 (d, 1H, J = 8.72 Hz, H-Ar), 7.72 (dd, 1H, J_1 = 2.33 Hz, J_2 = 6.68 Hz, H-Ar), 7.60 (d, 1H, J = 8.04 Hz, H-Ar), 7.52-7.47 (m, 2H, H-Ar), 7.39-7.30 (m, 3H, H-Ar), 7.19 (s, 2H, NH_2), 6.21 (s, 1H, CH) ppm; ^{13}C NMR (100 MHz, DMSO-d_6) δ_C 160.3,147.8, 137.3, 135.0, 134.3, 130.9, 130.6, 130.2, 130.1, 129.6, 128.9, 128.8, 127.3, 124.7, 122.3, 119.5, 116.5, 112.2, 52.5, 35.1 ppm.

RESULTS AND DISCUSSION

The description of composition, structure and morphology of the nanocatalysts is an important factor for predicting their catalytic performance. Therefore, in the first stage of this research, the structure of ZnO@zeolite-Y was identified by using different techniques such as FT-IR, FE-SEM, EDAX, BET and XRD. Then, the catalytic behavior of ZnO-modified zeolite was evaluated in the preparation of 4*H*-chromenes.

Heterostructured ZnO@zeolite-Y nanohybrids were synthesized through a hydrothermal reaction between the colloidal suspension of zeolite-Y and the solution of zinc chloride in an alkaline environment. Scheme 1 illustrates the synthesis of zeolite-Y supported zinc oxide nanoparticles. This process is performed according to the following reaction [38]. In order to evaluate the content of ZnO supported on zeolite-Y, atomic absorption spectroscopy (AAS) was used. The results revealed that the content of ZnO on zeolite was 0.566 mmol g^{-1} (46.1 ppm).

$$ZnCl_2 + 2NH_4OH \rightarrow Zn(OH)_2\downarrow + 2\ NH_4Cl$$

$$Zn(OH)_2 \rightarrow ZnO + H_2O$$

The morphology of zeolite-Y and ZnO@zeolite-Y nanocomposites was investigated by FE-SEM technique (Fig. 1). It can be seen that zeolite-Y has a crystalline structure in the form of chamfered edged cubes (Fig. 1a). Additionally, it is easy to find that the ZnO species have been supported on the surface of zeolite-Y with a good dispersion (Fig. 1b). As can be seen in Fig. 1c, the mean size of ZnO nanoparticles, formed by this process, was estimated to be 20-40 nm, which was graphically analyzed by the Digimizer software.

The EDX of the prepared ZnO@zeolite-Y nanocomposites is presented in Fig. 2. The presence of zinc atom is observed along with elements of zeolite in this hetero-structure. These results indicate that ZnO nanoparticles were successfully loaded on the zeolite-Y crystal.

The FT-IR spectra of the pure zeolite-Y and the prepared ZnO@zeolite-Y are illustrated in Fig. 3. In the zeolite-Y spectrum, the vibration bands at 3452 cm^{-1} and 1640 cm^{-1}

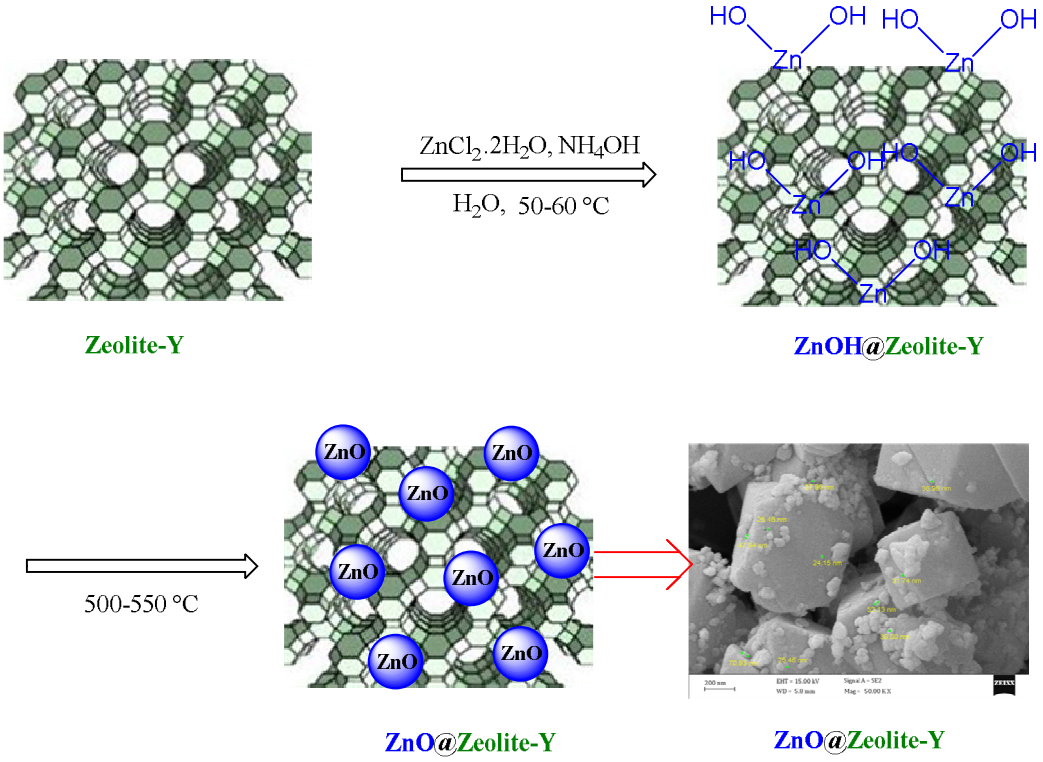

Scheme 1. The procedure for the synthesis of ZnO@zeolite-Y nanohybrids

are attributed to asymmetrical stretching of O-H (interporous H_2O molecules or O-H bonds) and the bending vibration of the H_2O molecule is appeared in 1421-1385 cm^{-1}. The intense band at 1020 cm^{-1} is corresponded to the stretching vibration of Si-O, and the bands at 577-460 cm^{-1} for Si-O-Si bending vibration and Al-O stretching vibration. Moreover, comparing the IR spectrum of the pure zeolite-Y and that of ZnO@zeolite-Y indicates that the decrease in peak intensity at wave number 3589 cm^{-1} is due to the formation of ZnO nanoparticles on the surface of zeolite and removal of H_2O inside the zeolite structure due to calcining operations [2,39]. Additionally, the Zn-O bond appears in 460 cm^{-1} and its intensity is slightly increased. The comparison of these two IR spectra (band at 577 cm^{-1}) also shows the structure of the final nanoporous product has been preserved [40].

Figure 4 shows the XRD patterns of pure zeolite-Y and the prepared ZnO@zeolite-Y. The XRD pattern of zeolite-Y matches with the Fa (JCDPS card no. 39-1380) that shows a crystalline structure with a typical face centered cubic (fcc) structure. The patterns of ZnO@zeolite peaks are mostly similar with the zeolite peaks that indicates the small compression of the Zeolite crystalline structure in the presence of ZnO nanoparticles without changing the cubic structure shape. Moreover, the characteristic XRD peaks of ZnO@zeolite-Y composite materials were displayed at 2θ 31.17º, 34.41º, 36.13º, 47.47º, 56.37º, 62.69º, and 68.49º which are assigned to the diffractions of the (100), (002), (101), (102), (110), (103), and (112) reflections, respectively. These peaks were related to the ZnO nanoparticles which were in accordance with ZnO (JCDPS card no. 80-0074) [4,37]. The crystal size of ZnO nanoparticles can be determined from the XRD pattern by using Debye-Scherrer's equation.

$$D(hkl) = \frac{0.94\lambda}{\beta \cos\theta}$$

where $D(hkl)$ is the average crystalline diameter, 0.94 is the Scherrer's constant, λ is the X-ray wavelength, β is the half width of XRD diffraction lines and θ is the Bragg's angle in degree. The crystal size of ZnO was calculated to be 43 nm.

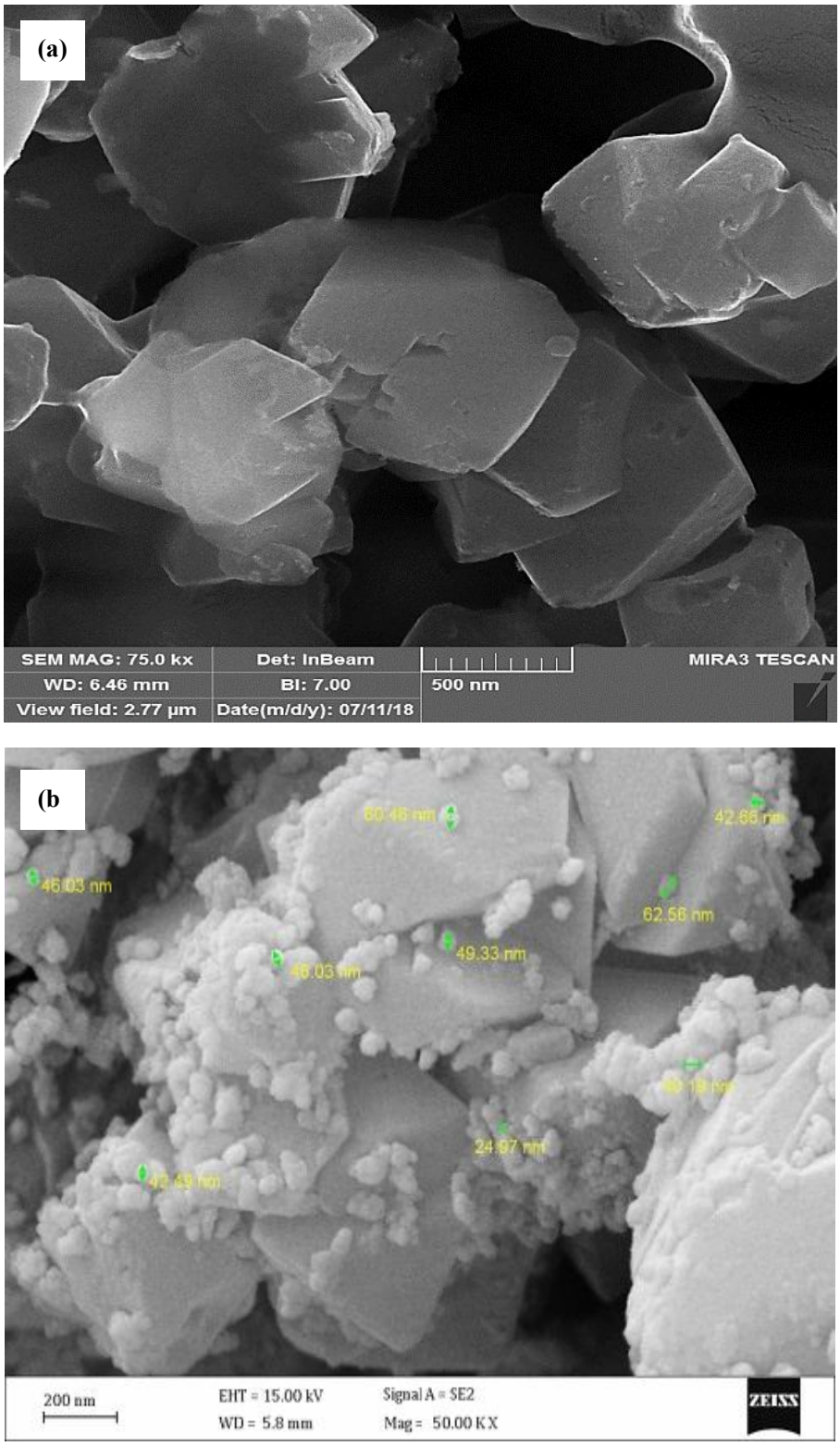

Fig. 1. (a) FE-SEM image of zeolite-Y, (b) ZnO@zeolite-Y nanomaterials and (c) histogram of the particles size distribution.

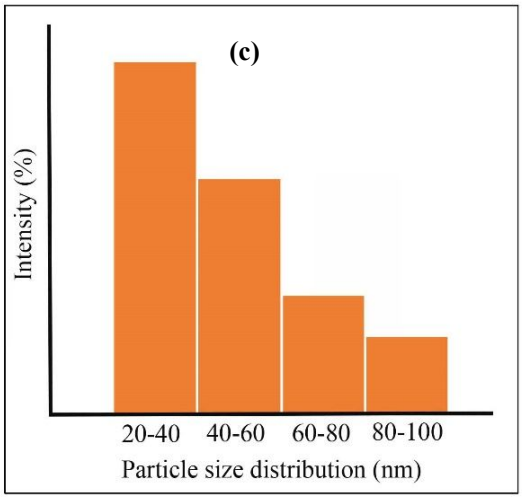

Fig. 1. Continued.

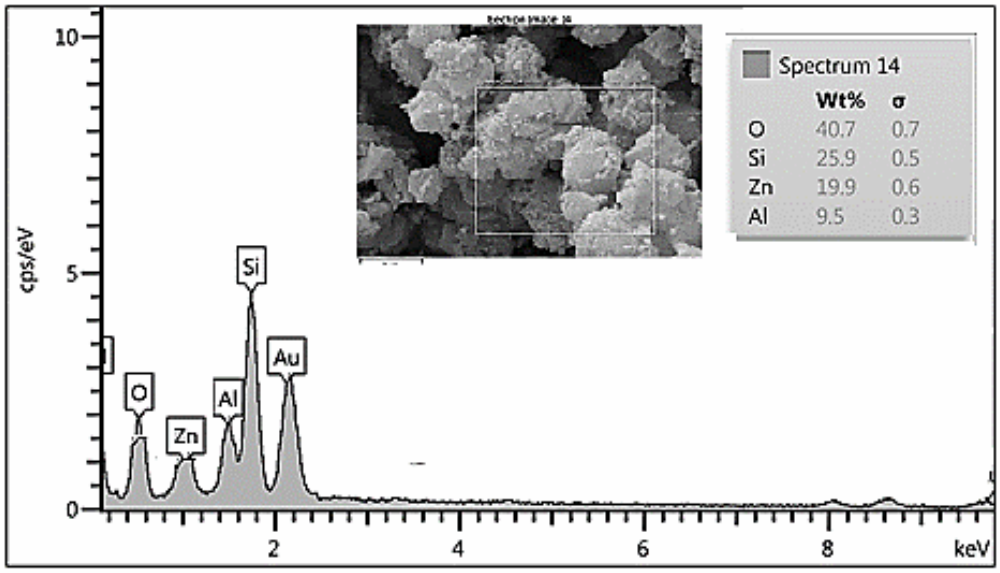

Fig. 2. EDX analysis of ZnO@zeolite-Y heterostructures.

The N_2 adsorption-desorption isotherm of zeolite-Y and ZnO@zeolite-Y are shown in Fig. 5. As can be seen, zeolite and metal-zeolite structures exhibit nitrogen types I isotherms which represents the microporous frameworks. The textural properties of zeolite structures are presented in Table 1. Comparison of S_{BET} from 619.66 m^2 g^{-1} for parent zeolite-Y to 639.42 m^2 g^{-1} for ZnO@zeolite-Y shows increase in specific surface after immobilization of ZnO. These results indicate that the ZnO nanoparticles phases formed a porous layer on the surface and in the channel of the zeolite-NaY structure. The modified zeolite-NaY has a lower pore volume in comparison with that of pure zeolite-Y as a result of filling the pores of zeolite with ZnO nanoparticle [39].

After identifying and verifying the structure of the prepared ZnO@zeolite-Y, the catalytic application of

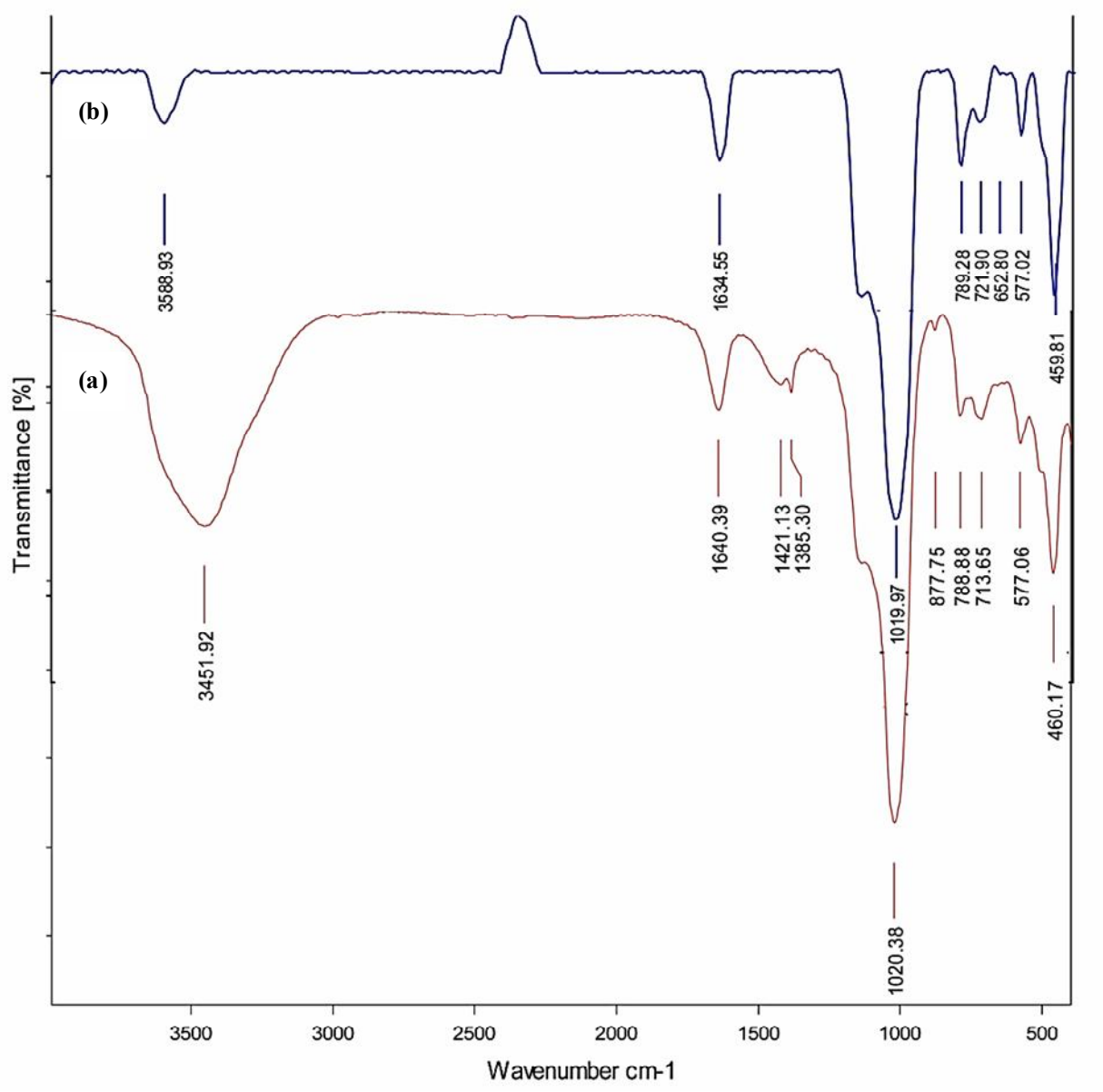

Fig. 3. FT-IR spectra of (a) zeolite-Y and (b) ZnO@zeolite-Y.

this nanohybrid was evaluated in the preparation of 4*H*-chromene derivatives (Scheme 2).

At the outset, benzaldehyde, *β*-naphthol, and malononitrile were chosen as model substrates under solvent-free conditions. The influence of quantity of nanocatalyst and the effect of temperature were studied to optimize the reaction conditions. Experimental results are reported in Table 2. As shown in this table, the model reaction without nanocatalyst resulted in the formation of product 4a in poor yields (Table 2, entry 1). The temperature is markedly influential on the rate of reaction. Therefore, to select the appropriate temperature, the reaction was checked in the temperature range from 60-120 °C with 0.05 g of catalyst. The isolated product yield obtained was 94% at 110 °C in 30 min (Table 2, entry 5). Determining the minimum amount of nanocatalyst is also necessary for optimization of the formation of product in every catalytic process. It was observed that the reaction yield improved

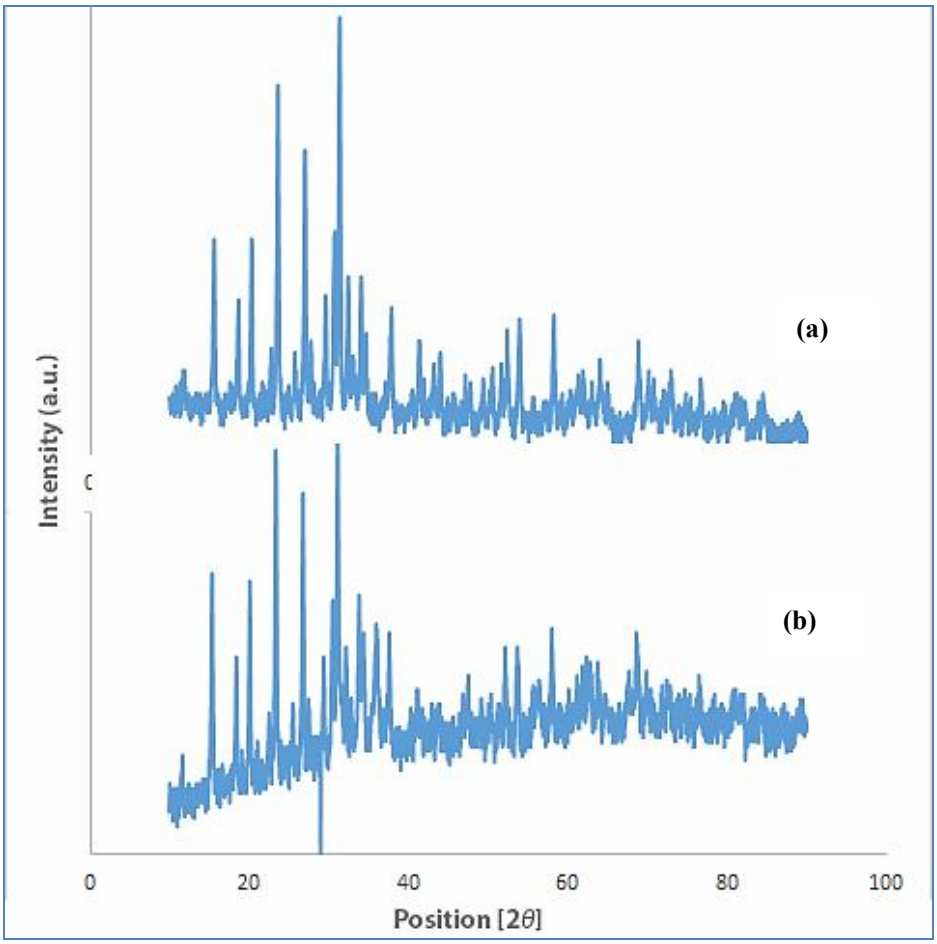

Fig. 4. XRD patterns of (a) pure zeolite-Y and (b) ZnO@zeolite-Y.

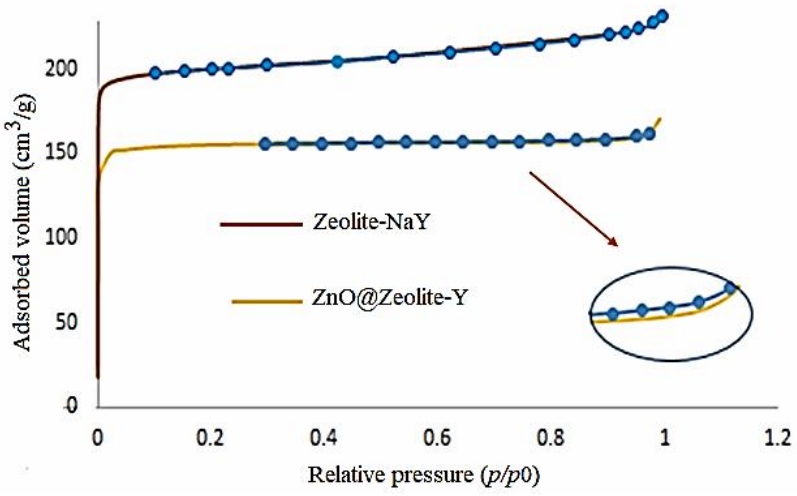

Fig. 5. N_2 adsorption/desorption isotherms of zeolite-Y and ZnO@zeolite-Y.

Table 1. Porosimetery Values for Zeolite-Y and its Functionalized Product

Material	S_{BET} ($m^2\ g^{-1}$)[a]	V_{BJH} ($cm^3\ g^{-1}$)[b]	D_{BJH} (nm)[c]	V_{HKM} ($cm^3\ g^{-1}$)[d]	M_{pd} (nm)[e]
Zeolite-Y	619.66	0.0667	4.84	0.3091	2.235
ZnO@zeolite-Y	639.49	0.0263	4.82	0.2417	2.645

[a]Specific surface area. [b]Pore volume. [c]Pore size (calculated from the adsorption branch). [d]Maximum pore volume at p/p° = 0.174699824 (estimated using the Horvath-Kawazoe method). [e]Mean pore diameter (4V/A by BET).

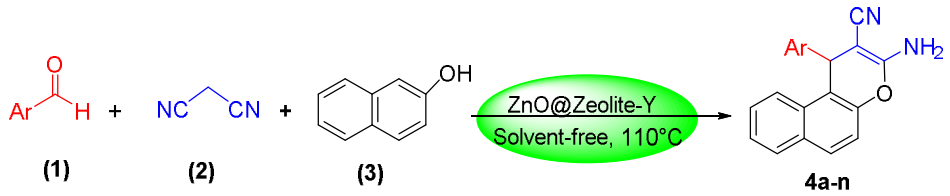

Scheme 2. Synthetic pathway of 2-amino-4*H*-chromenes

Table 2. Optimization of Reaction Conditions.

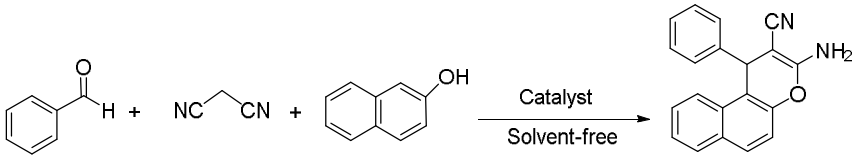

Entry	Catalyst (g)	Temperature (°C)	Time (min)	Yield (%)
1	-	110	180	30
2	ZnO@Z-Y (0.05)	60	100	80
3	ZnO@Z-Y (0.05)	90	50	83
4	ZnO@Z-Y (0.05)	110	30	94
5	ZnO@Z-Y (0.05)	120	30	94
6	ZnO@Z-Y (0.04)	110	45	88
7	ZnO@Z-Y (0.03)	110	50	82
8	ZnO@Z-Y (0.02)	110	70	60
9	ZnO@Z-Y (0.06)	110	30	93
10	ZnO (0.05)	120	220	40
11	Zeolite (0.05)	120	235	35

[a]Isolated yield.

Table 3. Synthesis of 2-Aamino-4*H*-chromene Derivatives Using Different Aldehydes

Entry	R	Product	Time (min)	Yield (%)[a]	M.p. (°C)	
					Obs.	Lit. [41]
1	C_6H_5	4a	30	94	280-282	279-280
2	4-Me-C_6H_4	4b	25	86	274-276	273-274
3	2-OMe-C_6H_4	4c	30	89	220-222	225-226
4	4-OMe-C_6H_4	4d	25	92	192-193	190-192
5	3,5-$(OMe)_2$-C_6H_3	4e	30	94	215-217	213-215
6	3-OMe,4-OH-C_6H_3	4f	25	85	250-252	252-253
7	4-OH-C_6H_4	4g	30	85	287-288	289-291
8	2-Cl-C_6H_4	4h	20	87	272-275	271-272
9	4-Cl-C_6H_4	4i	15	92	174-175	173-175
10	4-F-C_6H_4	4j	10	93	230-232	228-229
11	3-NO_2-C_6H_4	4k	10	95	234-236	235-236
12	4-NO_2-C_6H_4	4l	10	91	181-183	176-178
13	3-NO_2,4-Cl-C_6H_3	4m	10	84	176-179	181-183
14	2,6-Cl_2-C_6H_3	4n	40	80	206-208	-[42]

[a]Pure product isolated.

with increasing the amount of nanocatalyst from 0.02 to 0.06 g in shorter reaction time. By using 0.05 g, of catalyst, the yield rapidly enhanced to 94% in a short reaction time (30 min). ZnO as a basic catalyst and zeolite-Y as a weak acid catalyst were not very effective for this reaction. The product yields were 40 and 35%, respectively (Table 2, entries 10 and 11). Nanoscale and mesoporous support such as zeolite create catalysts with high surface are, high surface area, small crystallite size and more active sites, which can lead to the higher performance of the catalyst.

After optimizing the reaction conditions, in order to explore the scope and generality of this procedure, different aromatic aldehydes with electron-withdrawing or electron-releasing substituents were evaluated. The respective results are summarized in Table 3. The catalytic reaction proceeded with a variety of aldehydes in the presence of catalytic amounts of ZnO@zeolite at 110 °C and the desired products were obtained in good to excellent yields (84-95%) in relatively short reaction times, without formation of any side products. As can be seen in Table 3, the procedure was highly effective and the nature of substituent on the aromatic ring of aldehydes did not show obvious effects in terms of yields and times under the optimized conditions.

A mechanistic pathway for the catalytic synthesis of 4*H*-chromenes is presented in Scheme 3. ZnO@zeolite facilitates the Knoevenagel condensation through Lewis acid-Lewis basic catalyzed approach. The oxygen of carbonyl groups of benzaldehyde is activated by Zn^{2+} (Lewis acid active sites). Additionally, the deprotonation of C-H bond of malononitrile can occur in the presence of ZnO nanoparticles (O^{2-} of ZnO) acts as a Lewis basic catalyst and α-cyanocinnamonitrile forms as intermediate (I). Next,

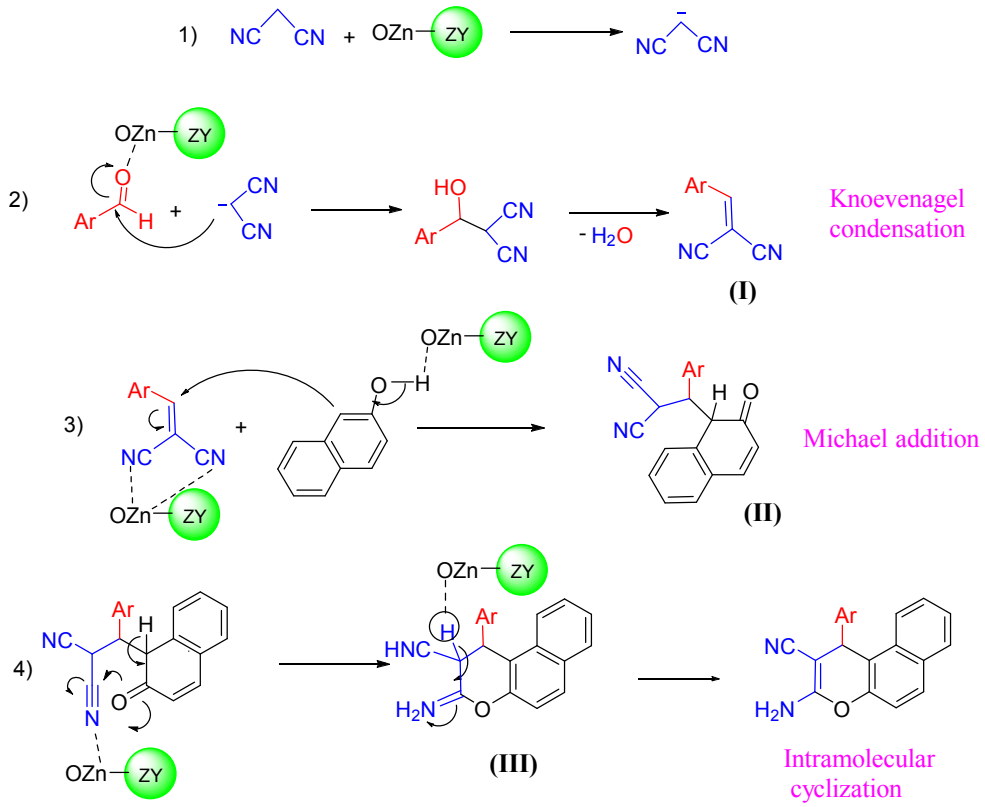

Scheme 3. Plausible mechanism for the synthesis of 4*H*-chromene

during the Michael addition reaction, nucleophilic attack on α-cyanocinnamonitrile occurs by 2-naphtol to give intermediate (II). Alternatively, further aromatization and cyclocondensation of spices (II) give intermediate (III) and finally it is converted to final product [41].

The reusability of the heterogeneous catalyst was investigated for the model reaction under the optimized conditions. After completion of the catalytic process, ZnO@zeolite was easily separated by using a simple filtration from the reaction mixture. It was washed with ethanol several times, dried in a vacuum oven and reused in the next reaction. The results of recyclability of the ZnO@zeolite experiments are shown in Fig. 6. No significant reduction in catalyst activity was observed after five times. The technique used in this study could be applied to the synthesis of other supported homogeneous catalysts along with prevention of agglomeration of heterogeneous nanocatalysts and easy separation. Therefore, the combination of ZnO nanoparticles and zeolite as an applicable support found to be an efficient catalytic nanosystem for this reaction. Also, the ZnO content of the recovered catalyst estimated by atomic absorption spectroscopy was 0.562 mmol g^{-1} (45.77 ppm). Therefore, no metal oxides leaching to the solution was observed.

Moreover, to show the advantages of using ZnO@zeolite catalyst in the synthesis 2-amino-4*H*-chromenes, this synthesis pathway was compared with literature resulted in reports of using various catalysts for the synthesis of 4k. As shown in Table 4, in the presence of this green and heterogeneous nanocatalyst, the results were better than other catalysts.

CONCLUSIONS

In conclusion, we have succeeded in the preparation and characterization of a zeolite-NaY supported ZnO nanoparticles and described a highly efficient and eco-friendly protocol *via* a one-pot three-component reaction for the synthesis of 2-amino-4*H*-chromene derivatives catalyzed by nano ZnO@zeolite under solvent-free media.

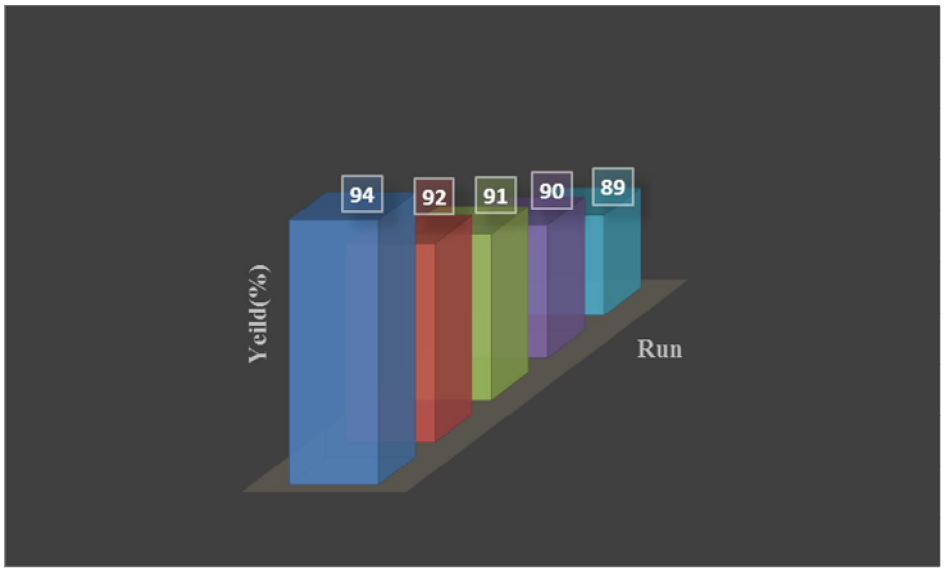

Fig 6. Recyclability chart of zeolite-Y supported ZnO nanoparticles.

Table 4. Comparison of ZnO@zeolite with other Catalysts Reported in the Literature for the Preparation of 4k

Entry	Catalyst	Amount; condition	Time (min)	Yield (%)	Ref.
1	1,4-Diazabicyclo[2.2.2]octane	0.0224 g; grinding, r.t.	30	95	[43]
2	$Y(NO_3)_3.6H_2O/SiO_2$	0.24 G; Water, reflux	2 h	80	[44]
3	[Amb]L-prolinate	0.08g; EtOH, reflux	30	87	[45]
4	Potassium hydrogen phthalate	25 mol%; Water, 50 °C	4.2 h	90	[46]
5	Potassium phtalimide	15 mol%; Water, reflux	10	89	[47]
6	Poly(4-vinylpyridine)	0.1 g; Solvent-free, 80 °C	10	89	[48]
7	Triethanolamine	0.1 ml; Solvent-free, 100 °C	10	92	[49]
8	PS-$[C_4(MIM_2][OH]_2$	0.04 g; Water, 80 °C	20	93	[50]
9	Nano-$TiCl_4.SiO_2$	0.1 g; Solvent-free, 90 °C	10	93	[51]
10	ZnO@zeolite	0.05 g; Solvent-free, 110 °C	10	95	This work

The present methodology offers noticeable advantages including shorter reaction time, high yields of the products, simplicity of the pathway, environmental safety of the process, ease of separation and recyclability of the nanocatalyst.

ACKNOWLEDGMENTS

We are grateful to the Payame Noor University for providing financial and technical supports for this work.

REFERENCES

[1] J. Liang, Z. Liang, R. Zou, Y. Zhao, Adv. Mater. 29 (2017) 1701139.

[2] a) G. Perot, M. Guisnet, J. Mol. Catal. 61 (1990) 173; b) C.G.S. Lima, N.M. Moreira, M.W. Paixão, A.G. Corrêa, Curr. Opin. Green Sustain. Chem. 15 (2019) 7.

[3] a) M.A. Aroon, A.F. Ismail, T. Matsuura, M.M. Montazer-Rahmati, A Review; Sep. Purif. Technol. 75 (2010) 229; b) E. Koohsaryan, M. Anbia, A Review; Chin. J. Catal. 37 (2016447; c) S. Chassaing, V. Bénéteau, P. Pale, Curr. Opin. Green Sustainable Chem. 10 (2018) 35.

[4] L. Zhao, Z.C. Liu, Z.F. Liu, Energy Mater. 10 (2015) 60.

[5] a) V. Rama, K. Kanagaraj, K. Pitchumani, J. Org. Chem. 76 (2011) 9090; b) M. Kalhor, N. Khodaparast, Res. Chem. Intermed. 41 (2015) 3235.

[6] A. Qurashi, M. Haffar, Z.H. Yamani, RSC Adv. 5 (2015) 22570.

[7] V.R. Batistela, L.Z. Fogac, S.L. Fávaro, W. Caetano, N.R. Fernandes-Machado, N. Hioka, Colloids Surf. A Physicochem. Eng. Asp. 513 (2017) 20.

[8] S.S. Katkar, P.H. Mohite, L.S. Gadekar, K.N. Vidhate, M.K. Lande, Chin. Chem. Lett. 21 (2010) 421.

[9] O. Sacco, V. Vaiano, M. Matarangolo, Sep. Purif. Technol. 193 (2018) 303.

[10] D. Singh, P. Patidar, A. Ganesh, S. Mahajani, Ind. Eng. Chem. Res. 52 (2013) 14776.

[11] A.A. Gabrienko, S.S. Arzumanov, A.V. Toktarev, I.G. Danilova, I.P. Prosvirin, V.V. Kriventsov, V.I. Zaikovskii, D. Freude, A.G. Stepanov, ACS Catal. 7 (2017) 1818.

[12] M. Wang, K.P. Rakesh, J. Leng, W.Y. Fang, L. Ravindar, D.C. Gowda, H. LiQin, Bioorg. Chem. 76 (2018) 113.

[13] B.B. Tour, D.G. Hall, Chem. Rev. 109 (2009) 4439.

[14] G.R. Green, J.M. Evans, A.K. Vong, In Comprehensive Heterocycl. Chem. II; A.R. Katritzky, C.W. Rees, E.F.V. Scriven, Eds.; Pergamon Press: Oxford. 5 (1995) 469.

[15] a) B.M. Rao, G.N. Reddy, T.V. Reddy, B.L.A. Prabhavathi Devi, R.B.N. Prasad, J.S. Yadav, B.V. Subba Reddy, Tetrahedron Lett. 54 (2013) 2466; b) B. Kazemi, S. Javanshir, A. Maleki, M. Safari, H.R. Khavasi, Tetrahedron Lett. 53 (2012) 6977; c) A. Maleki, S. Azadegan, Inorg. Nano-Met. Chem. 47 (2017) 917; d) A. Maleki, S. Azadegan, J. Inorg. Organomet. Polym. 27 (2017) 714; e) A. Maleki, M. Ghassemi, R. Firouzi-Haji, Pure Appl. Chem. 90 (2018) 387; f) A. Maleki, A.A. Jafari, S. Yousefi, Carbohydr. Polym. 175 (2017) 409; g) A. Maleki, H. Movahed, P. Ravaghi, Carbohydr. Polym. 156 (2017) 259.

[16] S.J. Mohr, M.A. Chirigos, F.S. Fuhrman, J.W. Pryor, Cancer Res. 35 (1975) 3750.

[17] K. Hiramoto, A. Nasuhara, K. Michiloshi, T. Kato, K. Kikugawa, Mutat. Res. 395 (1997) 47.

[18] G. Bianchi, A. Tava, Agric. Biol. Chem. 51 (1987) 2001.

[19] M.M. Khafagy, A.H. El-Wahas, F.A. Eid, A.M. El-Agrody, Farmaco 57 (2002) 715.

[20] C.P. Dell, C.W. Smith, Eur. Patent Appl. E.P. 537949, Chem. Abstr. 119 (1993) 139102d.

[21] D.R. Anderson, S. Hegde, E. Reinhard, L. Gomez, W.F. Vernier, L. Lee, S. Liu, A. Sambandam, P.A. Snider, L. Masih, Bioorg. Bioorg. Med. Chem. Lett. 15 (2005) 1587.

[22] J. Safari, Z. Zarnegar, J. Mol. Struct. 1072 (2014) 53.

[23] L. Chen, X.J. Huang, Y.Q. Li, M.Y. Zhou, W. Zheng, Monatsh. Chem. 140 (2009) 45.

[24] T.S. Jin, J.C. Xiao, S.J. Wang, T.S. Li, Ultrason. Sonochem. 11 (2004) 393.

[25] S.R. Kale, S.S. Kahandal, A.S. Burange, M.B. Gawande, R.V. Jayaram, Catal. Sci. Technol. 3 (2013) 2050.

[26] J. Safari, Z. Zarnegar, M. Heydarian, J. Taibah. Univ. Sci. 7 (2013) 17.

[27] M.M. Heravi, K. Bakhtiari, V. Zadsirjan, F.F. Bamoharram, Bioorg. Med. Chem. Lett. 17 (2007) 4262.

[28] M.J. Khurana, B. Nand, P. Saluja, Tetrahedron 66 (2010) 5637.

[29] Z. Zarnegar, J. Safari, New J. Chem. 40 (2016)7986.

[30] A. Pourkazemi A. Zare Org. Chem. Res. 2 (2016) 88.

[31] B. Şen, N. Lolak, Ö. Paral, M. Koca, A. Şavk, S.

Akocak, F. Şen, Nano-Struct. Nano-Object. 12 (2017) 33.

[32] J. Safari, M. Heydarian, Z. Zarnegar, Arab. J. Chem. 10 (2017) s2994.

[33] M. Khodajoo, S. Sayyahi, S.J. Saghanezhad, Russ. J. Gen. Chem. 86 (2016) 1177.

[34] A.F. Mahmoud, F.F.A. El-Latif, A.M. Ahmed, Chin. J. Chem. 28 (2010) 91.

[35] M. Kalhor, Org. Chem. Res. 2 (2015) 59.

[36] M. Kalhor, S. Banibairami, S.A. Mirshokraie, Green Chem. Lett. Rev. 11 (2018) 334.

[37] M. Kalhor, Z. Zarnegar, RSC Adv. 9 (2019) 19333.

[38] A. Kołodziejczak-Radzimsk, T. Jesionowski, A Review, Materials 7 (2014) 2833.

[39] A.A. Alswata, M.B. Ahmad, N.M. Al-Hada, H.M. Kamari, M.Z.B. Hussein, N.A. Ibrahim, Results Physics 7 (2017) 723.

[40] J. Perez-Pariente, J.A. Martens, P.A. Jacobs, Appl. Catal. 31 (1987) 35.

[41] A.R. Moosavi-Zare, M.A. Zolfigol, O. Khaledian, V. Khakyzadeh, M. Darestani Farahani, M.H. Beyzavi, H.G. Kruger, Chem. Eng. J. 248 (2014) 122.

[42] M. Esquivias-Pérez, E. Maalej, A. Romero, F. Chabchoub, A. Samadi, J. Marco-Contelles, M.J. Oset-Gasque, Chem. Res. Toxicol. 26 (2013) 986.

[43] A.S. Akandi, E. Balali, T. Mosavat, M.M. Ghanbari, A. Eazabadi, Oriental J. Chem. 30 (2014) 587.

[44] B. Karami, M. Farahi, M. Bazrafshan, S. Khodabakhshi, South African J.Chem. 67 (2014) 109.

[45] M. Keshavarz, N. Iravani, M.H. Ahmadi Azqhandi, S. Nazari, Res. Chem. Intermediate. 42 (2016) 4591.

[46] H. Kiyani, F. Ghorbani, Res. Chem. Intermediate. 41 (2015) 7847.

[47] H. Kiyani, F. Ghorbani, Chem. Pap. 68 (2014) 1104.

[48] J. Albadi, A. Mansournezhad, M. Darvishi-Paduk, Chin. Chem. Lette. 24 (2013) 208.

[49] B. Maleki, B. Baghayeri, S. Sheikh, S. Babaee, S. Farhadi, Russ. J. Gen. Chem. 87 (2017) 1064.

[50] F. Heidarizadeh, N. Taheri, Res. Chem. Intermediate. 42 (2016) 3829.

[51] B.B.F. Mirjalili, L. Zamani, K. Zomorodian, S. Khabnadideh, Z. Haghighijoo, Z. Malakotikhah, S.A. Ayatollahi Mousavi, S. Khojasteh, J. Mol. Struct. 1116 (2016) 102.